


Initial states for quantum field simulations in phase space

Peter D. Drummond ^{1,2} and Bogdan Opanchuk¹

¹*Swinburne University of Technology, Melbourne, Victoria 3122, Australia*

²*JILA, University of Colorado and National Institute of Standards and Technology, Boulder, Colorado 80309, USA*



(Received 19 May 2020; accepted 20 July 2020; published 25 August 2020)

Bosonic quantum fields and quantum devices can be simulated in phase space, to overcome exponential complexity issues as the Hilbert space dimensionality grows. Algorithms for sampling initial quantum states are analyzed here as a fundamental issue in these simulations. The generalized P , Wigner, and Q -function phase-space methods are treated, with applications ranging from Bose-Einstein condensates to quantum computers and photonic networks. Quantum initial conditions treated include multimode Gaussian states and general number state expansions. These are sampled probabilistically, in complex- P -distribution cases with additional complex weights. For high-order correlations of the type found in many quantum technology experiments, different representations and sampling techniques have a sampling error that changes exponentially as the mode number increases. Purely probabilistic techniques may scale exponentially worse than experimental shot-noise error scaling. Yet, combining random samples with complex weighting techniques gives error scaling that is equal or even exponentially better than experimental shot-noise scaling. We show that complex weighted P -distribution sampling can also be used to initialize simulations with the Wigner distribution, which is difficult to sample owing to its nonpositive character. As a result, complex weighted sampling can require exponentially less samples than either experiment or unweighted probabilistic sampling, leading to efficient simulation techniques for quantum networks and BECs.

DOI: [10.1103/PhysRevResearch.2.033304](https://doi.org/10.1103/PhysRevResearch.2.033304)

I. INTRODUCTION

For simulations of large dynamical quantum systems, one must have scalability as the mode number increases [1], since the number of dimensions in the Hilbert space is exponentially complex in the number of modes. Scalability is an issue even when there are exact solutions, because representing an arbitrary initial quantum state may require a superposition of exponentially many eigenstates. This is a severe limitation on dynamical calculations even in exactly soluble models [2]. Therefore probabilistic sampling is often essential for scalable computation.

To solve this problem, phase-space methods are widely used in large dynamical quantum simulations. Wigner [3] developed the first quantum phase-space method. Husimi [4] invented the first probabilistic representation, and Moyal [5] derived a dynamical theory. Glauber adapted these approaches to normally ordered operators in laser physics [6,7]. Such techniques were later extended [8] and used to simulate quantum fields in superfluorescence, pulsed quantum squeezing [9–11], and many other quantum processes [12].

These methods have already been used to treat very large Hilbert spaces, up to millions of qubit equivalents in BEC dynamics [13–15], and thousands of qubit equivalents [16–18] in the simulation of optical quantum computers, including the coherent Ising machine used to solve NP-hard optimization problems [19–21]. Both types of system can now be experimentally scaled to large sizes, with measured higher-order correlations [22–24].

Here we describe novel algorithmic approaches to simulating the initial quantum states of such dynamical simulations, using probabilistic sampling methods. In order to utilize phase-space representations, one must generate initial quantum states. For general initial states, complex weights are shown to be effective. These can greatly improve the efficiency of quantum simulations, with exponentially large improvements possible.

The methods described here can be used for different types of operator ordering. This includes normal ordered P representations, symmetrically ordered Wigner representations and antinormally ordered Q functions. These require different strategies for sampling, but also lead to quite different sampling errors, especially when higher-order moments and correlations are calculated.

Random sampling techniques in phase space for Gaussian initial quantum states are relatively simple to implement. The important case of initial number states is also treated here. Such cases are common in quantum information applications. There are existence theorems and random sampling methods for phase-space representations, which are explained.

Published by the American Physical Society under the terms of the Creative Commons Attribution 4.0 International license. Further distribution of this work must maintain attribution to the author(s) and the published article's title, journal citation, and DOI.

We show that complex weighting techniques are directly applicable, and give evidence for exponential reductions in sampling errors with mode number M for high-order correlations, compared both to direct probabilistic simulation and to the estimated sampling errors in experiments due to shot noise. The results are directly applicable to photonic networks. The sampling error e_S is directly proportional to $1/\sqrt{S}$ for S computed or experimentally measured random samples. As a result, both the computational and experimental time scales as $1/e_S^2$.

This exponential reduction in sampling errors we find in these complex weighted approaches therefore leads to exponentially *faster* simulation times for high-order correlations at large mode numbers.

II. PHASE-SPACE REPRESENTATIONS

We start by summarizing the properties of phase-space representations. The positive- P and truncated Wigner-Moyal phase-space methods have been employed to simulate one-dimensional (1D) quantum field dynamics in photonics [25] and in Bose-Einstein condensate (BEC) quantum dynamics in higher dimensions [26]. Both methods were also applied to full simulations of optical fibers, including Raman effects [27], with experimental verification of the quantum squeezing predictions [28–30].

Later applications included large-scale truncated Wigner simulations of BEC collisions [31], simulated quantum transport in a BEC in an optical lattice [32], detailed comparison of experiment and theory for optical fiber quantum correlations, to below the quantum noise level [33], comparisons of 3D positive- P and Wigner simulations of BEC collisions with 150 000 atoms from first principles [15], proposals for atomic Hong-Ou-Mandel correlations from BEC collisions [34], violations of Bell inequalities [35,36], and many other applications [12] including Boson sampling quantum computers [17,18]. Other applications include representations of parity operators, with existence and boundedness theorems summarized in recent literature [37].

A. Quantum and stochastic fields

We consider operator quantum fields $\hat{\psi}$ and $\hat{\psi}^\dagger$, which are non-Hermitian fields with bosonic commutation relations:

$$[\hat{\psi}(\mathbf{x}), \hat{\psi}^\dagger(\mathbf{x}')] = \delta(\mathbf{x} - \mathbf{x}'). \quad (1)$$

The number density operator is $\hat{n}(\mathbf{x}) = \hat{\psi}^\dagger(\mathbf{x})\hat{\psi}(\mathbf{x})$, and the total number operator in a volume V is

$$\hat{N} = \int_V \hat{n}(\mathbf{x}) dV. \quad (2)$$

The fields are expanded in annihilation and creation operators as

$$\begin{aligned} \hat{\psi}(\mathbf{x}) &= \sum_{n=1}^M u_n(\mathbf{x}) \hat{a}_n, \\ \hat{\psi}^\dagger(\mathbf{x}) &= \sum_{n=1}^M u_n^*(\mathbf{x}) \hat{a}_n^\dagger. \end{aligned} \quad (3)$$

This is an M -mode Hilbert space with a number-state basis of $|\mathbf{n}\rangle$, where $\mathbf{n} = (n_1, \dots, n_M)$. The Bose operators are $\hat{\mathbf{a}}$, where $\hat{\mathbf{a}} = (\hat{a}_1, \dots, \hat{a}_M)$. Extended vectors are defined as $\vec{\hat{\mathbf{a}}} = [\hat{\mathbf{a}}, \hat{\mathbf{a}}^\dagger]$, so that $\hat{a}_j^\dagger = \hat{a}_{j+M}$. In the equivalent phase-space representations, there is a progression of representations from normally ordered, to symmetrically ordered, then antinormally ordered approaches. The corresponding distributions have an increasing variance going from normal to antinormal ordering. These representations are called s -ordered, where $s = 0$ for normal ordering or P functions, $s = 1/2$ for symmetric ordering or W functions, and $s = 1$ for antinormal ordering or Q functions.

The quantum fields correspond to stochastic fields $\vec{\psi} = [\psi, \psi^+]$ in phase space [10,25]. In generalized P representations, ψ, ψ^+ are independent but conjugate in the mean, while $\psi^+ \equiv \psi^*$ in the classical-like Wigner and Q representations. Given an expansion of the quantum field with mode functions $u_n(\mathbf{x})$, one obtains

$$\begin{aligned} \psi(\mathbf{x}) &= \sum_{k=1}^M u_k(\mathbf{x}) \alpha_k, \\ \psi^+(\mathbf{x}) &= \sum_{k=1}^M u_k^*(\mathbf{x}) \beta_k. \end{aligned} \quad (4)$$

For an s -ordered representation, $n_s(\mathbf{x}) = \psi(\mathbf{x})\psi^+(\mathbf{x})$ is the s -ordered stochastic number density of the fields. Similarly, $n_k = \alpha_k \beta_k$ is the s -ordered stochastic mode occupation, where $\beta_k = \alpha_k^*$ in the Wigner and Q distributions. The relationship between quantum and stochastic number densities depends on the momentum cutoff, which defines a lattice cell volume ΔV .

We use $\langle \dots \rangle$ to denote a quantum operator expectation, and $\langle \dots \rangle_s$ an s -ordered stochastic average. If we define $\{O(\hat{\mathbf{a}}, \hat{\mathbf{a}}^\dagger)\}_s$ to be an s -ordered quantum moment, which in general could be normally ordered, symmetrically ordered or antinormally ordered, then this corresponds to an s -ordered phase-space average:

$$\langle O(\vec{\alpha}) \rangle_s \equiv \langle \{O(\vec{\alpha})\}_s \rangle. \quad (5)$$

This change in ordering means that one must include a correction factor when calculating either the number density $\hat{n}(\mathbf{x})$ or the mode occupation \hat{n}_k , so that

$$\begin{aligned} \langle \hat{n}(\mathbf{x}) \rangle &= \left\langle n_s(\mathbf{x}) - \frac{s}{\Delta V} \right\rangle_s, \\ \langle \hat{n}_k \rangle &= \langle n_k(\mathbf{x}) - s \rangle_s. \end{aligned} \quad (6)$$

On sampling an initial quantum state, the time-evolution depends on a quantum Hamiltonian. This gives rise to a functional Fokker-Planck equation for the stochastic fields $\vec{\psi}$, which can be transformed into stochastic partial differential equations (SPDE).

More general representations exist in which Gaussian operators are used as a basis for expanding fermionic or bosonic states [38–43]. These are outside the scope of this paper, but can also give efficient sampling. This can be seen from the graph of sampling errors, in Fig. 1, showing that Gaussian sampling requires a comparable number of samples to the best complex weighted P -function methods, although it has larger computational overheads.

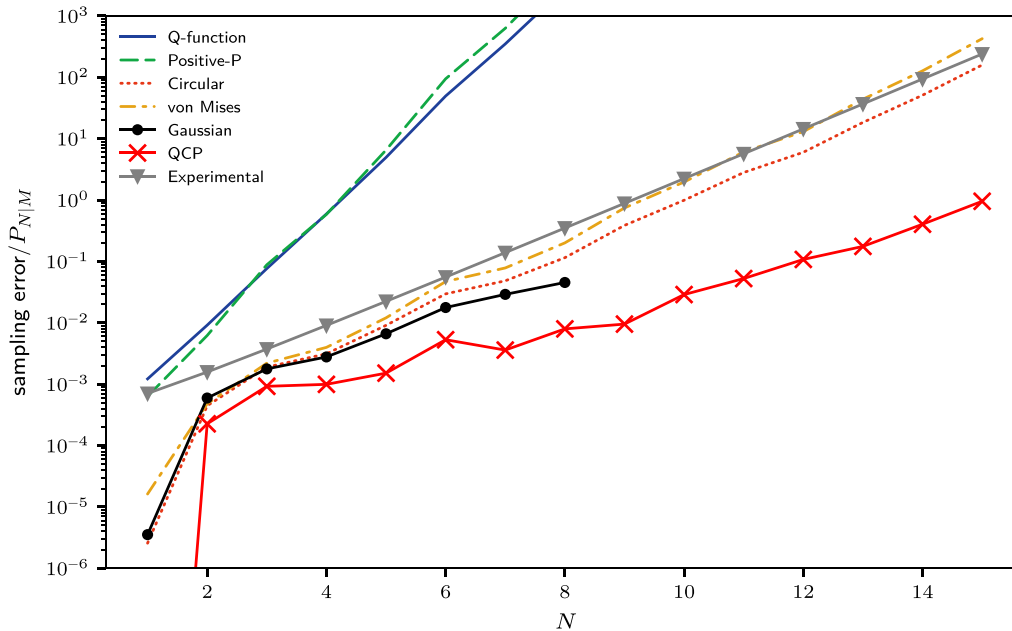


FIG. 1. Scaling of relative sampling error e_s versus total boson number N for N th-order Boson sampling correlations using different phase-space distributions. The upper two lines correspond to generating samples with the Q function and positive- P distributions. The middle two dotted and dashed lines correspond to different complex weighted sampling methods, namely circular and von Mises sampling. The bottom two lines are obtained using the QCP method and a Gaussian kernel representation. These show exponentially lower sampling errors than the other techniques, as the mode number $M = 2N$ and the total boson number N are increased. They also have a lower growth rate than even the experimental sampling errors for these high-order correlations. Sampling errors are averaged over five random unitaries with $S = 4 \times 10^6$ random samples for each unitary. The grey line shows estimated experimental sampling errors due to shot noise, $e_s = 1/\sqrt{S\langle P_{N|M} \rangle_U}$, for the same number of samples. Details given in Sec. V.

B. P representations

The normally ordered Glauber P representation [6] uses a diagonal coherent-state projector to expand the density matrix, but is singular for nonclassical fields. The generalized P representation [8] extends this by using an off-diagonal coherent projector to treat all quantum states without singularities. It is defined as a real or complex phase-space function $P(\vec{\alpha})$, such that

$$\hat{\rho} = \int P(\vec{\alpha}) \hat{\Lambda}(\vec{\alpha}) d\mu(\vec{\alpha}). \tag{7}$$

Here, $\vec{\alpha} = (\alpha, \beta)$ is a complex vector in a nonclassical phase space of $4M$ real phase-space dimensions, and $d\mu(\vec{\alpha})$ is an integration measure. This can either be a volume or surface measure in the enlarged phase space $\vec{\alpha}$. The result is an exact expansion of the quantum density matrix in terms of the coherent state projection operator

$$\hat{\Lambda}(\vec{\alpha}) = \prod_{j=1}^M \frac{|\alpha_j\rangle\langle\beta_j^*|}{\langle\beta_j^*|\alpha_j\rangle} = \prod_{j=1}^M \hat{\Lambda}_j(\alpha_j, \beta_j). \tag{8}$$

This projector is defined in terms of M -mode Bargmann-Glauber coherent states $|\alpha_j\rangle$ in each mode $j = 1, \dots, M$:

$$|\alpha\rangle \equiv e^{-|\alpha|^2/2} \sum_{n=0}^{\infty} \frac{\alpha^n}{\sqrt{n!}} |n\rangle. \tag{9}$$

The normalization factor for each mode projector is the inner product,

$$\langle\beta^*|\alpha\rangle = e^{\beta\alpha - |\alpha|^2/2 - |\beta|^2/2}. \tag{10}$$

A consequence of the definition is that the P function is normalized, which follows since $Tr(\hat{\rho}) = Tr(\hat{\Lambda}) = 1$, so that $\int P(\vec{\alpha}) d\mu(\vec{\alpha}) = 1$. There are existence theorems and explicit constructions for all quantum states, which exist for both complex and positive- P representations [8,44].

C. Complex- P representation

The most general case is a complex $P(\vec{\alpha})$. This is sometimes called the gauge P representation [45,46], as the complex weight term acts a stochastic gauge, allowing multiple equivalent representations and dynamical equations. The complex distribution can be expanded as $P(\vec{\alpha}) = \Omega(\vec{\alpha})P_+(\vec{\alpha})$, where $P_+(\vec{\alpha})$ is real, positive and normalized, so $P_+(\vec{\alpha})$ can be sampled with probabilistic techniques:

$$\int P_+(\vec{\alpha}) d\mu(\vec{\alpha}) = 1. \tag{11}$$

Here, $\Omega(\vec{\alpha})$ is a complex weight, which is typically chosen so that it has a nearly uniform modulus, $|\Omega(\vec{\alpha})| \sim 1$, to give efficient sampling. From these definitions, it has a mean value of unity:

$$\langle\Omega(\vec{\alpha})\rangle_+ \equiv \int \Omega(\vec{\alpha})P_+(\vec{\alpha}) d\mu(\vec{\alpha}) = 1. \tag{12}$$

It is convenient to define a weighted mean, which includes the complex weights, so that the s -ordered average for $s = 0$ is given by

$$\langle O(\vec{\alpha}) \rangle_0 \equiv \iint O(\vec{\alpha}) P(\vec{\alpha}) d\mu(\vec{\alpha}). \quad (13)$$

Averages in all P distributions correspond quantum-mechanically to normal-ordered quantum averages, denoted $\langle \dots \rangle$. These have creation operators like \hat{a}^\dagger ordered to the left, and if $O(\vec{\alpha})$ is a power series in $\vec{\alpha}$, then the following equivalence holds:

$$\langle O(\vec{\alpha}) \rangle_0 = \langle : O(\hat{a}, \hat{a}^\dagger) : \rangle. \quad (14)$$

The average $\langle \hat{O} \rangle \equiv \text{Tr}(\hat{O}\hat{\rho})$ is a standard quantum ensemble average with density matrix $\hat{\rho}$, and $\langle O \rangle_0$ indicates the P -function average with $s = 0$. When sampling the distribution with S samples, averages are obtained from samples of $\vec{\alpha}^{(n)}$ distributed with probability $P_+(\vec{\alpha}^{(n)})$, so that

$$\langle O(\vec{\alpha}) \rangle_0 = \lim_{S \rightarrow \infty} \frac{1}{S} \sum_{n=1}^S \Omega(\vec{\alpha}^{(n)}) O(\vec{\alpha}^{(n)}). \quad (15)$$

Although formally exact, when using this approach for quantum dynamical calculations the sampling error grows in time due to the enlarged phase space. In some cases, there are additional boundary term errors in phase space. This requires the use of additional stabilizing gauges which extend the time duration that can be usefully simulated [46–49].

D. Wigner representation

Other representations include the Wigner and Q representations. These correspond to symmetrically ordered and antinormally ordered operators, respectively. They can be written formally as convolutions of the generalized P function, extending a result of Cahill and Glauber [7]:

$$\begin{aligned} P_s(\vec{\alpha}) &= \left(\frac{1}{\pi s}\right)^M \int P(\vec{\alpha}_0) e^{-(\alpha - \alpha_0) \cdot (\alpha^* - \beta_0)/s} d\mu(\vec{\alpha}_0) \\ &= \left(\frac{1}{\pi s}\right)^M \langle e^{-(\alpha - \alpha_0) \cdot (\alpha^* - \beta_0)/s} \rangle_0. \end{aligned} \quad (16)$$

Here, $P_s(\vec{\alpha})$ is an s -ordered operator representation, while $\vec{\alpha}_0 = (\alpha, \beta)$, corresponding to the $s = 0$ case with normal ordering. The phase space $\vec{\alpha}$ is classical, with $\vec{\alpha} \equiv [\alpha, \alpha^*]$. As defined above, $s = 1/2$ corresponds to symmetric ordering, and $s = 1$ to antinormal ordering. This is related to the Cahill-Glauber s_{CG} ordering parameter [7] by $s_{CG} = 1 - 2s$. One can define the original Glauber-Sudarshan P representation as the singular limit of the convolution in the limit of $s \rightarrow 0$. This may exist only as a generalized function, depending on the quantum state. Therefore we use the generalized P distribution $P(\vec{\alpha})$ on a nonclassical phase space for $s = 0$, so that all relevant cases can be treated without singularities.

There are multiple ways to define the Wigner representation. One way is as a convolution, given above. Thus a delta-function P representation representing a coherent state corresponds to a Gaussian Wigner function. For the case of the Wigner function one has $s = 1/2$, so that $P_{1/2}(\vec{\alpha}) \equiv W(\vec{\alpha})$. The Wigner function is always nonsingular and real. This representation is also generally nonpositive [50], making direct

probabilistic sampling impossible except for special cases, or by using weighted sampling methods with nonpositive weights.

Typically, the Wigner dynamical equations are truncated using an $1/N$ expansion for N bosons, in order to obtain tractable stochastic equations. This approach is approximately valid in a large particle number limit [26,51]. Averages are defined as integrals over the Wigner function, so if $d\vec{\alpha}$ is the complex phase-space volume integral, corresponding to $2M$ real dimensions, then

$$\langle O(\vec{\alpha}) \rangle_{1/2} \equiv \iint O(\vec{\alpha}) W(\vec{\alpha}) d\vec{\alpha}. \quad (17)$$

Just as with the P function, one can also define a weighted version, so that, if $W_+(\vec{\alpha})$ is defined as a positive probability, then $W(\vec{\alpha}) = \Omega(\vec{\alpha}) W_+(\vec{\alpha})$.

Other methods for direct sampling are available in the cases where $W(\alpha)$ is positive, but for pure states these are always Gaussian, unless approximations are used. The double-dimension formalism of the positive- P method is also applicable here, if we define a positive Wigner function on an extended phase space $\vec{\alpha} = [\alpha, \beta]$ [52].

E. Q function

The Q function, originally proposed by Husimi [4], is defined either using the convolution method, or directly using the fundamental definition that

$$Q(\vec{\alpha}) = \frac{1}{\pi^M} \langle \alpha | \hat{\rho} | \alpha \rangle. \quad (18)$$

As with the Wigner case, the extended vector $\vec{\alpha}$ is applicable if one defines $\vec{\alpha} = [\alpha, \alpha^*]$. For the case of the Q function one has $s = 1$, so that $P_1(\vec{\alpha}) \equiv Q(\vec{\alpha})$. The Q function is always nonsingular, real and positive. Direct probabilistic sampling is therefore possible. This method is also applicable, with some modifications, to qubits and fermions [43,53], and has been used for simulating large-order correlations and Bell violations [54,55].

Averages are defined as integrals over the Q function, so if $d\vec{\alpha}$ is the complex phase-space volume integral, corresponding to $2M$ real dimensions, then

$$\langle O(\vec{\alpha}) \rangle_1 \equiv \iint O(\vec{\alpha}) Q(\vec{\alpha}) d\vec{\alpha}. \quad (19)$$

While the Q function is positive, it does not generally have a normal stochastic process because the corresponding diffusion equation is not positive-definite. Instead, it is a stochastic process that propagates both forward and backwards in time [56–58], requiring specialized techniques to solve it. However, with relatively strong damping, conventional stochastic methods may still be approximately useful, as the corresponding diffusion matrix is then almost always positive definite [59].

III. INITIAL STATE REPRESENTATIONS

Quantum simulations require an efficient strategy for sampling a range of suitable initial conditions. In this section, we review some of the standard methods of initial quantum state representations, together with more efficient approaches using

complex weights and contour integrals. The combined choice of both representation and sampling method can make a large difference in simulation results, as it changes the sampling errors.

This is demonstrated in Fig. 1, which plots the sampling error for six different types of boson sampling simulations. In the graph, an N th-order output correlation is computed for N single photon inputs to an M -mode photonic network which implements a unitary transformation on the inputs. The relative sampling errors of different algorithms are compared to the experimental sampling error due to shot noise, with the same number of samples.

This is a very important point. A simulation technique with sampling errors that grow faster than experimental errors cannot be usefully scaled to a large size. To a first approximation, either a computation or an experiment takes a time proportional to the number of samples needed to obtain useful statistics. Predicting experimental results requires that the computational error is no larger than experimental errors. Hence, if the simulation technique takes exponentially longer than experiment to achieve the required sampling error, it will take too long to be useful at large scales. For high-order correlations, $+P$ and Q function methods using pure probabilities have sampling errors exponentially larger than experiment, circular and von Mises weighted methods have similar errors, and the QCP and Gaussian algorithms have errors that are exponentially lower than experiment. The representations and sampling methods used are explained below.

A. Gaussian states

It is straightforward to represent the phase-space distributions described above if the initial conditions are Gaussian states. Examples of these include coherent states [6], squeezed states [60], Bogoliubov states [32,61,62], and thermal states.

In all of these cases, sampling can be obtained in an s -ordered representation by generating N_g real Gaussian noises defined so that

$$\langle w_i w_j \rangle = \delta_{ij}, \quad (20)$$

together with corresponding random phase-space samples where $\vec{\alpha} = [\alpha_1, \dots, \alpha_{2M}]$, such that

$$\alpha_i = \alpha_i^0 + B_{ij} w_j. \quad (21)$$

Here the quantum mean value is given by $\langle \hat{a}_i \rangle_Q = \alpha_i^0$.

In order to randomly sample a Gaussian state with an s -ordered cross-correlation of $\{\hat{a}_i \hat{a}_j\}_s$, where $i, j = 1, \dots, 2M$ to include the entire extended vector of $2M$ annihilation and creation operators, one must obtain

$$\{\{\hat{a}_i \hat{a}_j\}_s\} = \alpha_i^0 \alpha_j^0 + \sigma_{ij}. \quad (22)$$

To obtain this, simply choose the $2M \times N_g$ complex square root \mathbf{B} , such that

$$\sigma_{ij} = \sum_{k=1}^N B_{ik} B_{jk}. \quad (23)$$

There are restrictions on \mathbf{B} for the Wigner and Q functions. The condition that $\alpha_j^* = \alpha_{M+j}$ implies that

$$B_{ik}^* = B_{i+M,k}. \quad (24)$$

In some ‘‘quasi-Gaussian’’ states, like a laser or a BEC, the true quantum states have no well-defined phase [63]. In such cases, one can generate a Gaussian state relative to some phase-reference amplitude, then randomize the phase.

If the dynamics and the final measurements are phase-independent, as is often the case, the last step of phase-averaging is not required: it does not change the results. In these cases, a coherent state is equivalent to a Poissonian average over number states, and either type of input can be used [62] with identical results for phase-independent measurements.

B. P distributions for number state expansions

In many cases, one wishes to sample the phase space for a number state, or a superposition of number states. This is particularly important in quantum information applications, where number states often occur as part of a quantum information or quantum computing protocol such as Boson sampling, which will be used as a benchmark for comparisons.

These are often more difficult to sample than Gaussian states. Quantum states can be characterized by their matrix elements in a number state basis such that $C_{nm} = \langle \mathbf{n} | \hat{\rho} | \mathbf{m} \rangle$:

$$\hat{\rho} = \sum_{nm} C_{nm} |\mathbf{n}\rangle \langle \mathbf{m}|. \quad (25)$$

For a number state mixture, all the off-diagonal terms vanish, and

$$\hat{\rho} = \sum_n C_n |\mathbf{n}\rangle \langle \mathbf{n}|. \quad (26)$$

This general approach has been used in simulations of boson sampling equivalent to permanents as large as 100×100 [17,18,64], with sampling errors that scale exponentially better than experimental sampling errors. It has also been applied to simulations of BEC quantum dynamics of solitons in one dimension, with initial quantum number states [65]. This technique was described previously, and is reviewed in greater detail here.

There are techniques explicitly developed to treat qudit Hilbert spaces, in which numbers of particles are bounded [66–68]. However, due to the effects of beam-splitters, photonic networks do not maintain a bounded number per mode. This is because even if each mode has at most a single particle initially, this bound is not maintained throughout the network. Many-particle states can be created in a single mode through beam-splitting [69]. Therefore it is simpler to use infinite dimensional Hilbert-space representations. As a result, we focus here on treating number state inputs to photonic or other bosonic networks, using methods that allow the particle number per mode to change dynamically.

For general states, the Glauber P distribution is typically singular. However, the generalized P distribution $P(\vec{\alpha})$ always exists as a probability distribution with a volume measure. It is not unique, but at least one positive distribution always exists [8] as

$$P(\vec{\alpha}) = \left[\frac{1}{4\pi} \right]^M e^{-|\alpha - \beta^*|^2/4} Q\left(\frac{\alpha + \beta^*}{2} \right). \quad (27)$$

This is not the most numerically efficient choice for sampling, since it is less compact than the Q function when obtained from this construction. Sampling is rather straightforward, based on an initial Q -function sample, and is described in the next section where the Q function case is treated.

While one can obtain a sample of any quantum state using the positive- P representation [70], we will show that other techniques using complex weight factors have greatly reduced sampling errors for computation of high-order correlations with states of low photon number. Since these states are often found in quantum technology applications, this is a very important consideration for practical quantum simulations.

C. Complex- P distribution expansions

Choosing the complex- P representation instead of the positive distribution in Eq. (27) adds a complex weight to the initial condition, which permits a more compact phase-space distribution, while still allowing the usual propagation equations for subsequent time evolution.

We therefore focus on the complex- P distribution, which is more compact than the positive- P distribution [8], but less well-known. The relevant existence theorem states that, for an expansion of an arbitrary density matrix in number states such that $C_{nm} = \langle \mathbf{n} | \hat{\rho} | \mathbf{m} \rangle$, and for circular contours enclosing the origin in each amplitude, then by Cauchy's theorem,

$$P(\vec{\alpha}) = \left(\frac{-1}{4\pi^2} \right)^M e^{\alpha \cdot \beta} \sum_{\mathbf{n}, \mathbf{m}} C_{nm} \prod_{k=1}^M \frac{\sqrt{n_k! m_k!}}{\alpha_k^{m_k+1} \beta_k^{n_k+1}}. \quad (28)$$

Here, \mathbf{n} and \mathbf{m} are summed over all combinations of integer occupation numbers, and the expansion of the density matrix is defined in the complex- P representation as

$$\hat{\rho} = \iint d\alpha d\beta P(\vec{\alpha}) \hat{\Lambda}(\vec{\alpha}). \quad (29)$$

For vacuum states, the simplest complex or positive- P function sample is simply one of a single point, $\alpha_k = \beta_k = 0$. For nonvacuum inputs one can use a circular contour of radius r_k and make a transition to polar coordinates, so that $\alpha_k = r_k \exp(i\phi_k^{(\alpha)})$, $\beta_k = r_k \exp(i\phi_k^{(\beta)})$, and similarly $d\alpha_k = i\alpha_k d\phi_k^{(\alpha)}$ and $d\beta_k = i\beta_k d\phi_k^{(\beta)}$.

As a result, the expansion becomes

$$\hat{\rho} = \int \cdots \int_0^{2\pi} d\vec{\phi} P^\phi(\vec{\phi}) \hat{\Lambda}(\vec{r} e^{i\vec{\phi}}), \quad (30)$$

where $\vec{\phi} \equiv (\phi^{(\alpha)}, \phi^{(\beta)})$, and the phase distribution quasiprobability is given by

$$P^\phi(\vec{\phi}) = \left(\frac{1}{2\pi} \right)^{2M} e^{\alpha \cdot \beta} \sum_{\mathbf{n}, \mathbf{m}} C_{nm} \prod_k \frac{\sqrt{n_k! m_k!}}{\alpha_k^{m_k} \beta_k^{n_k}}. \quad (31)$$

The radius r_k is chosen to minimize the sampling error. Typically this requires choosing $r_k^2 \lesssim \bar{n}_k$, where \bar{n}_k is the mean boson number. Samples are then generated along the contour, to give a Monte Carlo sampled contour integral, as explained in the next subsection. During time evolution, the generated samples of $\vec{\alpha}$ are needed together with weight factors, so the radius only needs to be specified initially.

This choice of r_k is based on empirical evidence, but there is a good physical reason for doing this that one can understand intuitively. By using $r_k^2 \lesssim \bar{n}_k$, one includes just the coherent states whose mean particle number is equal to the actual mean particle number. This greatly reduces the sampling of states whose contribution will cancel, thus improving the sampling error; reducing the radius further is beneficial for high-order correlations.

While this expansion is always applicable, we now assume for simplicity that we can choose the mode basis that defines the mode operators such that the initial density matrix factorizes with $\hat{\rho} = \prod \hat{\rho}_k$. For such multiple independent modes, a complex- P representation is defined as

$$P^\phi(\vec{\phi}) = \prod_{k=1}^M P_k^\phi(\vec{\phi}_k). \quad (32)$$

D. Classical and nonclassical phase

The complex- P representation phase variables can be understood intuitively on defining

$$\begin{aligned} \phi_k &= (\phi_k^{(\alpha)} - \phi_k^{(\beta)})/2, \\ \theta_k &= \phi_k^{(\alpha)} + \phi_k^{(\beta)}, \end{aligned} \quad (33)$$

where ϕ_k is the classical phase and θ_k is a nonclassical phase. This is only required to be nonzero when the quantum state has nonclassical features. Otherwise, one can choose a Glauber P function in which $\alpha_k = \beta_k^*$ and $\theta_k = 0$.

Expressing the phase-space variables in terms of the two types of phase, one has the result that

$$\begin{aligned} \alpha_k^{n_k} &= e^{im_k(\theta_k/2 + \phi_k)} r_k^{n_k}, \\ \beta_k^{m_k} &= e^{im_k(\theta_k/2 - \phi_k)} r_k^{m_k}. \end{aligned} \quad (34)$$

For the k th mode, the exponential term in Eq. (28) becomes $\exp(\alpha_k \beta_k) = \exp(r^2(\cos \theta_k + i \sin \theta_k))$. As a result, from Eq. (29), the phase quasiprobability can be expanded as

$$P_k^\phi = \sum_{nm} C_{nm}(\phi) I_k^{nm}(\theta). \quad (35)$$

We define $C_{nm}(\phi_k) = e^{-i(n_k - m_k)\phi_k} C_{nm}/2\pi$ and $\bar{n}_k = (n_k + m_k)/2$, with $I_k^{nm} = 0$ for $n_k = m_k = 0$. For other cases, the expansion coefficient I_k^{nm} is given by

$$I_k^{nm}(\theta) = \frac{\sqrt{n! m!}}{2\pi r_k^{n+m}} e^{(r_k^2 \cos \theta + i(r_k^2 \sin \theta - \bar{n}_k \theta))}. \quad (36)$$

More general cases with coherences between the modes can be treated, and lead to additional phase-coherence terms in the contour integral sampling.

E. One-photon example

As an example, consider a one-mode, one-photon state where $C_{nm}^{(1)}(\phi) = \delta_{n1} \delta_{m1}/2\pi$. Choosing $r_k = 1$, the only relevant term in Eq. (36) is

$$I^{11}(\theta) = \frac{1}{2\pi} e^{(\cos \theta + i(\sin \theta - \theta))}. \quad (37)$$

It then follows that the full expansion of the density matrix is given by

$$\hat{\rho}^{(1)} = \int_{-\pi}^{\pi} \frac{d\phi}{2\pi} \int_{-\pi}^{\pi} \frac{d\theta}{2\pi} e^{(\cos\theta + i(\sin\theta - \theta))} \hat{\Lambda}(\alpha, \beta). \quad (38)$$

It is instructive to verify that this is the correct expansion, noting that because of the normalization factors in (10), one finds that only diagonal terms with $n = m$ remain after integrating over ϕ , and the expansion can be rewritten as

$$\begin{aligned} \hat{\rho}^{(1)} &= \sum_n \int_{-\pi}^{\pi} \frac{d\theta}{2\pi n!} e^{i(n-1)\theta} |n\rangle\langle n|. \\ &= |1\rangle\langle 1|. \end{aligned} \quad (39)$$

This is as expected for a single-photon density matrix.

IV. CONTOUR SAMPLING TECHNIQUES

The expansions above are analytic, and random sampling techniques for contour integrals are treated in this section. We consider four possible sampling methods, each with their own domains of applicability.

A. QCP and circular sampling

In order to keep the simulation as compact as possible, we first consider the special case of taking $r \rightarrow 0$. This is very efficient for computing N th-order correlations of number states with N input particles, as found in boson sampling experiments, together with the restriction that $n_k = 0, 1$. We refer to this as QCP sampling. In this case,

$$P^\phi(\vec{\phi}) = \left(\frac{1}{2\pi}\right)^{2M} \Omega(\vec{\phi}). \quad (40)$$

In this limit, the averaging becomes a pure, unweighted phase average, so that the probability is uniform with $\mathcal{P}(\vec{\phi}) = (2\pi)^{-2M}$. The weight function, on the other hand, for each single photon input, is

$$\Omega_k(\vec{\phi}) = r_k^{-2} e^{-i(\phi_k^{(\alpha)} + \phi_k^{(\beta)})}. \quad (41)$$

Each nonvacuum input generates a random phase variable $\vec{\alpha} = r \exp(i\vec{\phi})$, with an arbitrarily small radius r . For a linear network, the output only depends on the phases, as the radius term is the same for all nonvanishing amplitudes. The radius term in the weight function cancels when calculating N th-order correlations, and so the calculation is independent of r for $r \rightarrow 0$. This is the most efficient way to sample N th-order correlations, but it is less useful for more general applications.

In the circular sampling method, the probability is again uniform with $\mathcal{P}(\vec{\phi}) = (2\pi)^{-2M}$. As in the QCP approach, one simply chooses two uniform random vectors, $\phi^\alpha \in [-\pi, \pi]^M$ and $\phi^\beta \in [-\pi, \pi]^M$. However, with this method, the radius is chosen such that $r_k = \sqrt{n_k}$. From Eq. (28), the corresponding complex weight factor is

$$\Omega(\vec{\phi}) = e^{\alpha\beta} \sum_{n,m} C_{nm} \prod_{kl} \frac{\sqrt{n_k! m_l!}}{\alpha_k^{n_k} \beta_k^{m_k}}. \quad (42)$$

With this algorithm, the modulus of the weight factor varies substantially with the phase for $n \gg 1$. As a result, this is not an efficient technique for a large particle number.

B. von Mises sampling

To obtain greater sampling efficiency over a range of input states, after transforming to classical and nonclassical phase variables ϕ and θ as described above, one can separate the real and imaginary parts of the exponential terms in (35), and use random probabilistic sampling from the real part, so that for modes with $n_k > 0$:

$$P_k(\alpha, \beta) d\alpha d\beta = \mathcal{P}_k(\phi, \theta) \Omega_k(\phi, \theta) d\phi d\theta. \quad (43)$$

This is a general expression for the case of factorized mode distributions treated above. Here $\Omega_k(\phi, \theta)$ is a complex weight factor, while $\mathcal{P}_k(\phi, \theta) \propto |\alpha\beta P_k(\alpha, \beta)|$. The normalization of the resulting real and positive probability $\mathcal{P}_k(\phi, \theta)$ is defined such that

$$\int d\theta d\phi \mathcal{P}_k(\phi, \theta) = 1. \quad (44)$$

To illustrate this general sampling procedure, we now suppose that each mode has an input number state. As a result, if P_k is the single-mode distribution for mode k with n_k bosons:

$$P_k(\alpha, \beta) = \begin{cases} \left(\frac{1}{2\pi i}\right)^2 \frac{n_k! e^{\alpha\beta}}{(\alpha\beta)^{n_k+1}} & \text{for } n_k > 0, \\ \delta(\alpha)\delta(\beta) & \text{for } n_k = 0. \end{cases} \quad (45)$$

Here, ϕ and θ are defined as in the previous subsection. For the number state case, the functions $\mathcal{P}_k(\phi, \theta)$ and $\Omega_k(\phi, \theta)$ are independent of ϕ , although this is not the case in general. Once the phase angles are randomly chosen according to this probability function, the imaginary part in the exponential of Eq. (36) generates an additional complex weight, Ω_k . Starting from the main result obtained above, Eq. (35), we find that the normalized probability distribution \mathcal{P}_k and complex weight Ω_k for the subset of modes with nonvacuum inputs are:

$$\begin{aligned} \mathcal{P}_k &= \frac{1}{4\pi^2 I_0(r^2)} \exp(r^2 \cos \theta_k), \\ \Omega_k &= \frac{n_k! I_0(r^2)}{r^{2n_k}} \exp(i(r^2 \sin \theta_k - n_k \theta_k)). \end{aligned} \quad (46)$$

The θ distribution, $2\pi \mathcal{P}_k(\theta_k)$, is the well-known circular von Mises distribution (\mathcal{V}) [71], defined as $\mathcal{V}(\theta|0, r^2) \equiv \exp(r^2 \cos \theta) / (2\pi I_0(r^2))$. The normalization of this distribution is provided by a modified Bessel function of the first kind of order zero, $I_0(x)$, while $\theta_k \in [-\pi, \pi)$ and $\phi_k \in [-\pi, \pi)$. This corresponds to sampling the phase variables independently as $\phi_k \sim \mathcal{U}(-\pi, \pi)$, and $\theta_k \sim \mathcal{V}(0, r^2)$, where \mathcal{U} is the uniform distribution.

From each sample, we calculate the phase-space variables as $\alpha_k = r \exp(i(\phi_k + \theta_k/2))$, $\beta_k = r \exp(i(\phi_k - \theta_k/2))$, where the von Mises sampling of θ can be obtained using well-known and efficient algorithms [72], which are available in the public domain [73].

For either circular or von Mises sampling, we use the delta-function distribution $P_k(\alpha_k, \beta_k) = \delta(\alpha_k)\delta(\beta_k)$ for vacuum modes where $n_k = 0$, that is, one takes $\alpha_k = \beta_k = 0$.

The samples are then used to calculate any moment $f(\alpha, \beta)$ in conjunction with the S drawn samples of α and β as

$$\langle f(\alpha, \beta) \rangle_P = \frac{1}{S} \sum_{j=1}^S \Omega(\alpha^{(j)}, \beta^{(j)}) f(\alpha^{(j)}, \beta^{(j)}). \quad (47)$$

where $\Omega = \prod \Omega_k$ is the total weight of the trajectory.

C. Large particle number sampling

It is generally optimal in terms of sampling efficiency to choose $r_k^2 \lesssim n_k$. For larger particle numbers, these expressions simplify, because one can use a large radius for the integration contour. The von Mises phase distribution asymptotically becomes a standard Gaussian of width $1/r$ in the limit of large r , and one can use the asymptotic Bessel function result that

$$I_0(z) = \frac{e^z}{\sqrt{2\pi z}} + O\left(\frac{1}{z}\right). \quad (48)$$

The sampled probability distribution for modes with nonzero inputs is then a uniform circular distribution in ϕ_k of $1/(2\pi)$, multiplied by a normalized Gaussian, so that

$$\mathcal{P}_k(\phi_k, \theta_k) \approx \frac{r_k}{(2\pi)^{3/2}} \exp(-r_k^2 \theta_k^2 / 2). \quad (49)$$

In the same large radius limit, the complex weight Ω_k can be calculated using Stirling's approximation. Introducing $n! = n^n \sqrt{2\pi n} e^{-n} (1 + O(1/n))$ and taking $r_k^2 = n_k$, one then obtains for the k th complex weighting term:

$$\begin{aligned} \Omega_k &\approx \frac{n_k! I_0(r_k^2)}{r_k^{2n}} \exp(i(r_k^2 \sin \theta_k - n_k \theta_k)), \\ &\approx \exp(in_k(\sin \theta_k - \theta_k)). \end{aligned} \quad (50)$$

Therefore it follows that $\Omega_k \approx \exp(-in_k \theta_k^3 / 6)$ to leading order. Noting that $\langle \theta_k^2 \rangle = 1/n_k$ in this approximation, and hence: $n_k \theta_k^3 \sim 1/\sqrt{n_k}$, these are relatively small phase factors. The mean value of the complex weight term is given by

$$\langle \Omega_k \rangle \approx \langle 1 - in_k \theta_k^3 / 6 - n_k^2 \theta_k^6 / 72 \rangle, \quad (51)$$

where one can show that $\langle \theta_k^6 \rangle = 15/n_k^3$.

As a result, in this approximation the overall mean weight factor is $\langle \Omega_k \rangle \approx 1 - 15/(72n_k)$, while it should be $\langle \Omega \rangle = 1$, if the exact von Mises distribution was used. This approximation error of order $1/n_k$ can be removed by including higher-order corrections of $O(1/n_k)$, if greater accuracy is required.

V. S-ORDERED DISTRIBUTIONS AND APPLICATIONS

There are several ways to sample the Wigner and Q functions, and we will describe two possibilities here. The first method is a direct sampling based on known analytic forms of the function, while the second method is convolution sampling based on the generalized P distribution as a starting point. Positive- P distribution sampling is also explained, and a comparison of several methods is made for a test case of a Boson sampling quantum computer.

A. Wigner and Q distributions

One can obtain an analytic form of the Wigner function in terms of associated Laguerre functions [7,74]. In the case of a factorized $\hat{\rho}$, which is diagonal in the number basis, this gives

$$W(\vec{\alpha}) = e^{-2|\alpha|^2} \sum_n C_n \prod_k \frac{2(-1)^{n_k}}{\pi} \mathcal{L}_{n_k}(4|\alpha_k|^2). \quad (52)$$

From this result, we can see that while the Wigner function always exists for any quantum state, it has no generally positive form, and in fact the negative-going part is often used to signify a quantum Schrodinger cat state [74,75]. High-order Laguerre functions are difficult to calculate numerically, owing to underflow, overflow, and round-off problems. Sampling them is also nontrivial, as they are extremely oscillatory. As a result, this approach is not usually employed for carrying out simulations, and convolution methods can provide better results for sampling Wigner functions [76].

Q function sampling is simpler, as this is always positive. For a number state n , one obtains that [7]

$$Q(\vec{\alpha}) = \prod_m \frac{|\alpha_m|^{2n_m}}{\pi n_m!} e^{-|\alpha_m|^2}. \quad (53)$$

This is essentially a product of gamma distributions, for which efficient sampling methods are known [77].

B. Positive- P distribution sampling

Given a random sample α_Q of the Q function, one can always obtain a random sample $\vec{\alpha}$ of the positive- P distribution by making use of the existence theorem, Eq. (27). A Q -function sample is used for the mean, $\alpha_Q = \vec{\alpha} = (\alpha + \beta^*)/2$, which is combined with a Gaussian sample for the difference, $\delta = (\alpha - \beta^*)/2$.

This shows that one can obtain an unweighted sample by taking a random complex sample δ with a Gaussian distribution such that $\langle |\delta_j|^2 \rangle = 1$ and defining

$$\begin{aligned} \alpha &= \alpha_Q + \delta, \\ \beta &= \alpha_Q^* - \delta^*. \end{aligned} \quad (54)$$

However, this seldom the most compact and efficient possible algorithm. For example, in a vacuum state, $\langle \hat{a} \hat{a}^\dagger \rangle = \langle |\alpha_Q|^2 \rangle = 1$ and the corresponding normally ordered positive- P moment is

$$\langle \hat{a}^\dagger \hat{a} \rangle = \langle \alpha \beta \rangle_P = 0. \quad (55)$$

In vacuum state it is therefore always more efficient to take $\alpha = \beta = 0$, which reduces the sampling error to zero, since the samples then have a zero variance.

C. Convolution sampling

We will now show, by using a different technique, that sampling the full Wigner distribution is possible, even for relatively complex quantum states. These techniques have proved useful in establishing the properties of the Wigner function when a full-scale simulation of a quantum Schrodinger cat transfer in optomechanics [76] was carried out using a complex- P distribution, which is an exact method.

The results given in Eq. (16) for convolutions of the P function imply that this is a general sampling theorem. Both $Q(\vec{\alpha})$ and $W(\vec{\alpha})$ can always be obtained using sampling methods provided that an algorithm for sampling the generalized P function is known, since a convolution is equivalent to adding a random gaussian variable. In the present case, one must also take into account that the convolution includes a dimensional reduction from a nonclassical phase space.

For s -ordered sampling, the fundamental convolution involves a complex weight of form:

$$\left(\frac{1}{\pi s}\right)^M e^{-(\alpha-\alpha_0)\cdot(\alpha^*-\beta_0)/s}. \tag{56}$$

One can use this weight directly [76]. Alternatively, to sample either the Wigner or Q function, we first define the following linear combinations:

$$\alpha_{\pm} = \frac{1}{2}(\alpha_0 \pm \beta_0^*). \tag{57}$$

The variable α_+ is equivalent to a ‘classical’ coordinate, while α_- indicates the degree of nonclassicality. To construct a real Gaussian convolution, if we define $\Delta = \alpha - \alpha_+$ and $i\delta = \Delta \cdot \alpha_-^* - \Delta^* \cdot \alpha_-$, then

$$(\alpha - \alpha_0) \cdot (\alpha^* - \beta_0) = |\Delta|^2 - |\alpha_-|^2 + i\delta. \tag{58}$$

The distribution is therefore a Gaussian convolution with a shift of Δ , and a complex weight, so that

$$W(\vec{\alpha}) = \left(\frac{1}{\pi s}\right)^M \iint P(\vec{\alpha}_0)\Omega_c(\vec{\alpha}, \vec{\alpha}_0)e^{-|\Delta|^2/s}d\mu(\vec{\alpha}_0), \tag{59}$$

where the complex weight function is $\Omega_c(\vec{\alpha}, \vec{\alpha}_0) = \exp[(|\alpha_-|^2 - i\delta)/s]$. Thus, one can sample the P function to obtain $\vec{\alpha}$, then sample the convolution variable, $\Delta_k = \Delta_k^x + i\Delta_k^y$ as $2M$ real Gaussian variables each with variance $s/2$, where $k = 1, \dots, M$. For fixed $\vec{\alpha}_0$, the variances in each quadrature are

$$\langle(\Delta_k^x)^2\rangle_s = \langle(\Delta_k^y)^2\rangle_s = \frac{s}{2}, \tag{60}$$

and the resulting phase-space coordinate of $\alpha = \alpha_+ + \Delta$ is a Wigner or Q function sample. However, when calculating ensemble averages with a generalized P distribution having a weight Ω_P as the starting point, an additional complex weight must be included with $\Omega_W = \Omega_P \exp[(|\alpha_-|^2 - i\delta)/s]$. While Ω_W is a complex weight, its average is real, and it is easily proved that $\langle\Omega_W\rangle = \langle\Omega_P\rangle = 1$. This exponential weight factor becomes increasingly large for nonclassical states $\vec{\alpha}_0$ with large $|\alpha_-|^2$. As a result, one must use a compact representation for the generalized P function. These compact contour representations are treated in previous sections.

D. Application to quantum networks

After obtaining a representation of the initial quantum state, quantum dynamical evolution in phase space can take place via a number of methods based on the Hamiltonian. Free-field evolution is the simplest case, although even this is essentially equivalent to calculating a matrix permanent, which is an exponentially hard problem.

For all types of linear evolution, with a Hamiltonian of

$$\hat{H}_0 = \hbar \sum_{i,j} \omega_{ij} \hat{a}_i^\dagger \hat{a}_j, \tag{61}$$

one finds that this simply involves a unitary matrix transformation U acting on α and β , leading to outputs $\alpha' = U\alpha$ and $\beta' = U^*\beta$. Correlations are obtained from moments of transformed samples α', β' . An N channel correlation, with a normally ordered representation, is

$$P_{N|M} = \left\langle \prod_{k=1}^N (\hat{a}'_k)^\dagger \hat{a}'_k \right\rangle = \left\langle \prod_{k=1}^N \alpha'_k \beta'_k \right\rangle_P. \tag{62}$$

In some guided wave experiments, there is no need to consider free-field evolution, provided waveguide dispersion and pulse shaping effects are negligible. In such cases the calculation of evolution is simply a question of multiplying by the relevant unitary matrix.

Nevertheless, the calculation of high-order correlations given number state inputs is highly nontrivial. It is in the $\#P$ class of computational complexity, as it is equivalent to computing a matrix permanent. It is also of substantial experimental interest as a diagnostic for a Boson sampling quantum computer [20,23,78]. Simulating this provides a useful testbed for comparisons of methods given above [17,18].

It is not surprising that sampling errors of high-order correlations increase with correlation order. Fortunately, complex weighting leads to an exponentially large relative decrease in sampling errors compared to other methods, as shown in Fig. 1. This graphs the relative sampling error for a computational simulation of the probability of a correlated output, given five random unitary transformations of N single boson inputs for $M = 2N$ possible input channels. The graph gives the relative sampling error in calculating an N th-order correlation function for a single count in each of N different predetermined output channels, using 4×10^6 random samples.

Here, six different phase-space representations are compared, with both complex weights and pure probabilities. Even with $N = 7$ bosons, the improvement in sampling error provided by complex weighting methods compared to pure probabilities is a factor of 10^5 . For the same errors, the best complex weighting method, QCP, requires 10^{10} times fewer samples, and is therefore 10^{10} times faster than purely probabilistic methods. This ratio increases rapidly with particle and mode number.

The graph also compares this performance with an experimental measurement, with the comparison based on the number of measurements required for the same relative error. This is estimated from the expected number of counts, which is $S\langle P_{N|M}\rangle_U$, where S is the number of samples and $\langle P_{N|M}\rangle_U$ is the average coincidence probability for having a count in N specific channels out of M . Here the probability is averaged over all possible random unitaries U . Due to Poissonian statistics, the mean relative sampling error due to shot noise is $e_S = 1/\sqrt{S\langle P_{N|M}\rangle_U}$.

From the theory of random unitary matrices there is a known scaling law [64] for the Haar average output correlation of N singly excited modes amongst M channels,

which is

$$\langle P_{N|M} \rangle_U = \frac{(M-1)!N!}{(M+N-1)!}, \quad (63)$$

Figure 1 shows that the best computational algorithms have 10^2 times lower sampling errors than experimental shot-noise errors at $N \sim 14$. This indicates a speedup of up to $\sim 10^4$ for the same error performance as an experiment. However, the QCP approach is rather specialized, and the Gaussian expansion method, although giving an excellent error performance requires large computational resources. The von Mises sampling method is the most widely useful, as it scales no worse than experiment and has a general applicability.

Using these initialization algorithms, up to 100 modes each with single photon input states, together with 100th-order correlations in the output after unitary transformations and random phase noise, have also been simulated [18]. This is larger than the best current photonic technologies [79], indicating that these numerical techniques are suitable for simulating the performance of many quantum devices.

VI. CONCLUSIONS

This paper analyses initial conditions for simulating quantum field propagation with s -ordered phase-space methods. Probabilistic sampling leads to stochastic partial differential equations which can be solved numerically even in large Hilbert spaces. There is another, more subtle issue: the

generation of arbitrary initial quantum states, which has a strong influence on sampling error.

For initial Gaussian states, the initial sampling is straightforward. Complex weighting techniques using circular contours and the complex P representation are more efficient when the initial states are number states. This provides a route for sampling distributions for any quantum states with arbitrary ordering, using convolution sampling. Depending on the algorithm, the resulting sampling errors for high-order correlations can vary by many orders of magnitude, ranging from exponentially smaller than the shot-noise sampling error, to exponentially larger than experimental sampling errors.

In summary, we have treated initial conditions for quantum field simulations. A comparison is given between different approaches, showing that exponentially large improvements are possible in the sampling error of high-order correlation functions using complex weighted random trajectories. Such techniques can be used to simulate quantum field dynamics with a finite digital computer, and may be useful in analyzing future quantum computers and other quantum technologies.

ACKNOWLEDGMENTS

Discussions with King Lun Ng and Run Yan Teh are gratefully acknowledged. This work was funded in part by an Australian Research Council Discovery Grant, and by the Joint Institute for Laboratory Astrophysics through a Visiting Fellowship. The authors wish to thank NTT Research for their financial support.

-
- [1] R. P. Feynman, *Int. J. Theor. Phys.* **21**, 467 (1982).
 - [2] V. A. Yurovsky, B. A. Malomed, R. G. Hulet, and M. Olshanii, *Phys. Rev. Lett.* **119**, 220401 (2017).
 - [3] E. Wigner, *Phys. Rev.* **40**, 749 (1932).
 - [4] K. Husimi, *Proc. Phys. Math. Soc. Jpn.* **22**, 264 (1940).
 - [5] J. E. Moyal, *Math. Proc. Cambridge Philos. Soc.* **45**, 99 (1949).
 - [6] R. J. Glauber, *Phys. Rev.* **131**, 2766 (1963).
 - [7] K. E. Cahill and R. J. Glauber, *Phys. Rev.* **177**, 1882 (1969).
 - [8] P. D. Drummond and C. W. Gardiner, *J. Phys. A* **13**, 2353 (1980).
 - [9] F. Haake, H. King, G. Schröder, J. Haus, and R. Glauber, *Phys. Rev. A* **20**, 2047 (1979).
 - [10] S. J. Carter, P. D. Drummond, M. D. Reid, and R. M. Shelby, *Phys. Rev. Lett.* **58**, 1841 (1987).
 - [11] P. D. Drummond and J. H. Eberly, *Phys. Rev. A* **25**, 3446 (1982).
 - [12] P. D. Drummond and S. Chaturvedi, *Phys. Scr.* **91**, 073007 (2016).
 - [13] C. M. Savage, P. E. Schwenn, and K. V. Kheruntsyan, *Phys. Rev. A* **74**, 033620 (2006).
 - [14] K. V. Kheruntsyan, *Phys. Rev. A* **71**, 053609 (2005).
 - [15] P. Deuar and P. D. Drummond, *Phys. Rev. Lett.* **98**, 120402 (2007).
 - [16] T. Shoji, K. Aihara, and Y. Yamamoto, *Phys. Rev. A* **96**, 053833 (2017).
 - [17] B. Opanchuk, L. Rosales-Zárate, M. D. Reid, and P. D. Drummond, *Phys. Rev. A* **97**, 042304 (2018).
 - [18] B. Opanchuk, L. Rosales-Zárate, M. D. Reid, and P. D. Drummond, *Opt. Lett.* **44**, 343 (2019).
 - [19] J. P. Dowling, J. D. Franson, H. Lee, and G. J. Milburn, in *Experimental Aspects of Quantum Computing* (Springer, Boston, 2005), pp. 205–213.
 - [20] S. Aaronson and A. Arkhipov, *Theory Comput.* **9**, 143 (2013).
 - [21] Y. Yamamoto, K. Aihara, T. Leleu, K.-i. Kawarabayashi, S. Kako, M. Fejer, K. Inoue, and H. Takesue, *npj Quant. Info.* **3**, 1 (2017).
 - [22] T. Schweigler, V. Kasper, S. Erne, I. Mazets, B. Rauer, F. Cataldini, T. Langen, T. Gasenzer, J. Berges, and J. Schmiedmayer, *Nature (London)* **545**, 323 (2017).
 - [23] D. J. Brod, E. F. Galvão, A. Crespi, R. Osellame, N. Spagnolo, and F. Sciarrino, *Adv. Photonics* **1**, 034001 (2019).
 - [24] F. Flamini, N. Spagnolo, and F. Sciarrino, *Rep. Prog. Phys.* **82**, 016001 (2018).
 - [25] P. D. Drummond and A. D. Hardman, *Europhys. Lett.* **21**, 279 (1993).
 - [26] M. J. Steel, M. K. Olsen, L. I. Plimak, P. D. Drummond, S. M. Tan, M. J. Collett, D. F. Walls, and R. Graham, *Phys. Rev. A* **58**, 4824 (1998).
 - [27] P. D. Drummond and J. F. Corney, *J. Opt. Soc. Am. B* **18**, 139 (2001).
 - [28] M. Rosenbluh and R. M. Shelby, *Phys. Rev. Lett.* **66**, 153 (1991).
 - [29] J. Heersink, V. Josse, G. Leuchs, and U. L. Andersen, *Opt. Lett.* **30**, 1192 (2005).

- [30] J. F. Corney, J. Heersink, R. Dong, V. Josse, P. D. Drummond, G. Leuchs, and U. L. Andersen, *Phys. Rev. A* **78**, 023831 (2008).
- [31] A. A. Norrie, R. J. Ballagh, and C. W. Gardiner, *Phys. Rev. Lett.* **94**, 040401 (2005).
- [32] J. Ruostekoski and L. Isella, *Phys. Rev. Lett.* **95**, 110403 (2005).
- [33] J. F. Corney, P. D. Drummond, J. Heersink, V. Josse, G. Leuchs, and U. L. Andersen, *Phys. Rev. Lett.* **97**, 023606 (2006).
- [34] R. J. Lewis-Swan, in *Ultracold Atoms for Foundational Tests of Quantum Mechanics* (Springer International, Switzerland, 2016), pp. 45–55.
- [35] P. D. Drummond, B. Opanchuk, L. Rosales-Zárate, and M. D. Reid, *Phys. Scr.* **2014**, 014009 (2014).
- [36] L. Rosales-Zárate, B. Opanchuk, P. D. Drummond, and M. D. Reid, *Phys. Rev. A* **90**, 022109 (2014).
- [37] B. Koczor, F. v. Ende, M. de Gosson, S. J. Glaser, and R. Zeier, [arXiv:1811.05872](https://arxiv.org/abs/1811.05872).
- [38] A. M. Perelomov, *Generalized Coherent States and Their Applications*, Texts and Monographs in Physics (Springer, Berlin, 1986).
- [39] J. F. Corney and P. D. Drummond, *Phys. Rev. A* **68**, 063822 (2003).
- [40] J. F. Corney and P. D. Drummond, *J. Phys. A* **39**, 269 (2006).
- [41] J. F. Corney and P. D. Drummond, *Phys. Rev. B* **73**, 125112 (2006).
- [42] J. F. Corney and P. D. Drummond, *Phys. Rev. Lett.* **93**, 260401 (2004).
- [43] L. E. C. Rosales-Zárate and P. D. Drummond, *New J. Phys.* **17**, 032002 (2015).
- [44] P. D. Drummond and M. Hillery, *The Quantum Theory of Nonlinear Optics* (Cambridge University Press, Cambridge, 2014).
- [45] P. Deuar and P. D. Drummond, *Phys. Rev. A* **66**, 033812 (2002).
- [46] P. Deuar and P. D. Drummond, *J. Phys. A* **39**, 2723 (2006).
- [47] A. Gilchrist, C. W. Gardiner, and P. D. Drummond, *Phys. Rev. A* **55**, 3014 (1997).
- [48] P. Deuar and P. Drummond, *Comput. Phys. Commun.* **142**, 442 (2001).
- [49] P. Deuar and P. D. Drummond, *J. Phys. A* **39**, 1163 (2006).
- [50] A. Kenfack and K. Życzkowski, *J. Opt. B: Quantum Semiclassical Opt.* **6**, 396 (2004).
- [51] A. Sinatra, C. Lobo, and Y. Castin, *J. Phys. B* **35**, 3599 (2002).
- [52] S. E. Hoffmann, J. F. Corney, and P. D. Drummond, *Phys. Rev. A* **78**, 013622 (2008).
- [53] F. T. Arecchi, E. Courtens, R. Gilmore, and H. Thomas, *Phys. Rev. A* **6**, 2211 (1972).
- [54] M. D. Reid, B. Opanchuk, L. Rosales-Zárate, and P. D. Drummond, *Phys. Rev. A* **90**, 012111 (2014).
- [55] B. Opanchuk, L. Rosales-Zárate, M. D. Reid, and P. D. Drummond, *Phys. Lett. A* **378**, 946 (2014).
- [56] A. Altland and F. Haake, *Phys. Rev. Lett.* **108**, 073601 (2012).
- [57] P. D. Drummond and M. D. Reid, *Phys. Rev. Research* **2**, 033266 (2020).
- [58] P. D. Drummond, [arXiv:1910.00001](https://arxiv.org/abs/1910.00001).
- [59] R. Zambrini, S. M. Barnett, P. Colet, and M. San Miguel, *Eur. Phys. J. D* **22**, 461 (2003).
- [60] *Quantum Squeezing*, edited by P. D. Drummond and Z. Ficek (Springer-Verlag, Berlin, Heidelberg, New York, 2004).
- [61] J. Ruostekoski and A. D. Martin, *Quantum Gases: Finite Temperature And Non-Equilibrium Dynamics* (Imperial College Press, London, 2013), pp. 203–214.
- [62] K. L. Ng, R. Polkinghorne, B. Opanchuk, and P. D. Drummond, *J. Phys. A: Math. Gen.* **52**, 035302 (2019).
- [63] W. H. Louisell, *Quantum Statistical Properties of Radiation* (Wiley, New York, 1973), p. 528.
- [64] P. D. Drummond, B. Opanchuk, L. Rosales-Zárate, M. D. Reid, and P. J. Forrester, *Phys. Rev. A* **94**, 042339 (2016).
- [65] K. L. Ng, B. Opanchuk, M. D. Reid, and P. D. Drummond, *Phys. Rev. Lett.* **122**, 203604 (2019).
- [66] D. W. Barry and P. D. Drummond, *Phys. Rev. A* **78**, 052108 (2008).
- [67] P. D. Drummond and M. D. Reid, *Phys. Rev. A* **94**, 063851 (2016).
- [68] B. Koczor, R. Zeier, and S. J. Glaser, *Phys. Rev. A* **101**, 022318 (2020).
- [69] C. K. Hong, Z. Y. Ou, and L. Mandel, *Phys. Rev. Lett.* **59**, 2044 (1987).
- [70] M. Olsen and A. Bradley, *Opt. Commun.* **282**, 3924 (2009).
- [71] K. V. Mardia and P. E. Jupp, *Directional Statistics*, Wiley Series in Probability and Statistics (John Wiley and Sons, Chichester, 2000).
- [72] D. Best and N. I. Fisher, *J. R. Stat. Soc. Ser. C* **28**, 152 (1979).
- [73] T. E. Oliphant, *A Guide to NumPy* (Trelgol Publishing, USA, 2006), Vol. 1, p. 85.
- [74] R. Y. Teh, F.-X. Sun, R. E. S. Polkinghorne, Q. Y. He, Q. Gong, P. D. Drummond, and M. D. Reid, *Phys. Rev. A* **101**, 043807 (2020).
- [75] F.-X. Sun, Q. He, Q. Gong, R. Y. Teh, M. D. Reid, and P. D. Drummond, *Phys. Rev. A* **100**, 033827 (2019).
- [76] R. Y. Teh, S. Kiesewetter, P. D. Drummond, and M. D. Reid, *Phys. Rev. A* **98**, 063814 (2018).
- [77] L. Devroye, *Non-Uniform Random Variate Generation* (Springer-Verlag, New York, 1986).
- [78] S. Aaronson, *Proc. R. Soc. London A* **467**, 3393 (2011).
- [79] H. Wang, J. Qin, X. Ding, M. C. Chen, S. Chen, X. You, Y. M. He, X. Jiang, L. You, Z. Wang, C. Schneider, J. J. Renema, S. Höfling, C.-Y. Lu, and J. W. Pan, *Phys. Rev. Lett.* **123**, 250503 (2019).